The Hubble Catalog of Variables (HCV)

K. V. Sokolovsky[1,2,3], **A. Z. Bonanos**[1], **P. Gavras**[1], **M. Yang**[1],
D. Hatzidimitriou[4,1], **M. I. Moretti**[5,1], **A. Karampelas**[6,1],
I. Bellas-Velidis[1], **Z. Spetsieri**[1,4], **E. Pouliasis**[1,4], **I. Georgantopoulos**[1],
V. Charmandaris[1], **K. Tsinganos**[1], **N. Laskaris**[7], **G. Kakaletris**[7],
A. Nota[8,9], **D. Lennon**[10], **C. Arviset**[10], **B. C. Whitmore**[8], **T. Budavari**[11],
R. Downes[8], **S. Lubow**[8], **A. Rest**[8], **L. Strolger**[8] and **R. White**[8]

[1]IAASARS, National Observatory of Athens, Greece
email: kirx@noa.gr

[2]Sternberg Astronomical Inst. MSU, Moscow, Russia

[3]Astro Space Center, LPI RAS, Moscow, Russia

[4]Department of Physics, National and Kapodistrian University of Athens, Greece

[5]INAF-Osservatorio Astronomico di Capodimonte, Napoli, Italy

[6]American Community Schools of Athens, Halandri, Greece

[7]Athena Research and Innovation Center, Maroussi, Greece

[8]Space Telescope Science Institute, Baltimore, MD, USA

[9]European Space Agency, Research and Scientific Support Dept., Baltimore, MD, USA

[10]European Space Astronomy Centre, Madrid, Spain

[11]The Johns Hopkins University, Baltimore, MD, USA

Abstract. The Hubble Source Catalog (HSC) combines lists of sources detected on images obtained with the WFPC2, ACS and WFC3 instruments aboard the Hubble Space Telescope (HST) and now available in the Hubble Legacy Archive. The catalogue contains time-domain information for about two million of its sources detected using the same instrument and filter on at least five HST visits. The *Hubble Catalog of Variables* (HCV) aims to identify HSC sources showing significant brightness variations. A magnitude-dependent threshold in the median absolute deviation of photometric measurements (an outlier-resistant measure of light-curve scatter) is adopted as the variability detection statistic. It is supplemented with a cut in $\chi^2_{\rm red}$ that removes sources with large photometric errors. A pre-processing procedure involving bad image identification, outlier rejection and computation of local magnitude zero-point corrections is applied to the HSC light-curves before computing the variability detection statistics. About 52 000 HSC sources have been identified as candidate variables, among which 7,800 show variability in more than one filter. Visual inspection suggests that $\sim$70% of the candidates detected in multiple filters are true variables, while the remaining $\sim$30% are sources with aperture photometry corrupted by blending, imaging artefacts or image processing anomalies. The candidate variables have AB magnitudes in the range 15–27^m, with a median of 22^m. Among them are the stars in our own and nearby galaxies, and active galactic nuclei.

Keywords. Techniques: photometric, stars: variables: other

1. Introduction

The Hubble Source Catalog (HSC; Whitmore *et al.* 2016, Budavári & Lubow 2012) combines individual source lists derived from images obtained with the WFPC2, ACS and WFC3 cameras aboard the HST. The source lists are created with SExtractor (Bertin & Arnouts 1996) from stacked images combining individual exposures taken within one

HST visit by using AstroDrizzle (Hack *et al.* 2012). Image stacking and source list extraction are performed as part of the routine processing in the Hubble Legacy Archive (Jenkner *et al.* 2006, Whitmore *et al.* 2008). As the accuracy of astrometric solutions associated with original HST images is limited by the positional accuracy of individual star positions in the Guide Star Catalog (Lasker *et al.* 2008), the HSC is cross-matched with the deep catalogues of Pan-STARRS, 2MASS and SDSS, and reached a typical absolute astrometric accuracy of $< 0''.1$; the Gaia catalogue will be used to increase further the accuracy of absolute astrometry in future HSC releases. The HSC sources are distributed in isolated pencil beams covering about 0.1% of the sky. For each detected source the HSC reports aperture photometry results based on published instrument zero-points as described in http://hla.stsci.edu/hla_faq.html. The HSC photometric precision, estimated from repeated measurements of the same sources, is about $0^m.02$–$0^m.04$.

One of the primary science goals of the HST is to improve the accuracy of the extra-galactic distance scale (Czerny *et al.* 2018) by observing standard candles like Cepheids (Freedman *et al.* 2001), supernovæ (Riess *et al.* 2018) and Mira variables (Huang *et al.* 2018). Some fields were observed during multiple HST visits in order to obtain very deep mosaic images (Koekemoer *et al.* 2013), perform astrometric studies (e.g. Anderson & van der Marel 2010, Nascimbeni *et al.* 2014), and calibration (Bellini *et al.* 2011). The HCV project aims to use the time-domain information from the HSC to perform a uniform variability search in the fields visited multiple times by the HST.

This talk summarised our variability detection technique, and presented the results of our preliminary variability search. Previous reports on the state of the HCV project have been given by Gavras *et al.* (2017), Sokolovsky *et al.* (2017b), Yang *et al.* (2017).

2. Pre-Processing and Variability Detection

The HSC data are grouped naturally in clusters of sources detected in spatially over-lapping images. For all sources in such a group we extracted light-curves from each instrument/filter combination with which the particular area of the sky was observed. A set of light-curves in one group obtained with the same instrument and filter is our basic variability search unit. The data quality criteria and variability detection thresholds are determined independently for each such unit.

Prior to conducting a variability search we try to improve the quality of the input photometric data. The first step is to apply quality cuts to discard sources marked as saturated, and detected less than a specified number of times (currently 5) with the given instrument and filter (so the light-curves of all the sources considered have at least the specified number of points). We reject groups where fewer than 300 sources pass the quality cuts in all instrument–filter combinations, as smaller samples are less well suited for the statistical analyses to be performed.

We assign a weight to each light-curve point using the 'synthetic error' – a combination of the estimated photometric error, the magnitude difference between the two concentric apertures of a different diameter ('concentration index'), the magnitude difference between the circular and automatically selected elliptical aperture tuned to the source size (SExtractor parameter 'MAG_AUTO'), and the offset distance from the matching position. Elevated values of any of those parameters may indicate that the source is blended, or affected by an uncleaned cosmic ray or other imaging artefact. For each light-curve we perform a weighted robust linear fitting. Light-curve points deviating from this fit, or ones with high values of the synthetic error, are flagged as outliers. Visits resulting in a high percentage of outliers ($> 20\%$) are identified as 'bad', and all measurements corresponding to such visits are discarded.

The second pre-processing step is the calculation and application of local magnitude zero-point corrections (e.g., Nascimbeni *et al.* 2014) that minimise the impact of
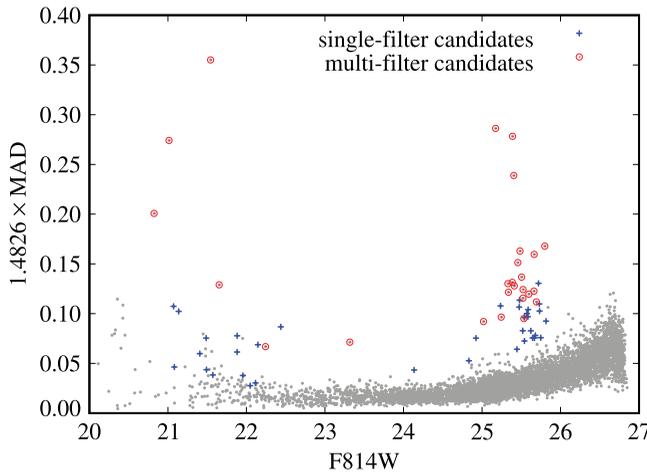
Figure 1. Median absolute deviation (scaled to σ of the Gaussian distribution) as a function of F814W magnitude for a field in the halo of M 31 originally investigated by Brown *et al.* (2004). The plot highlights candidate variables selected using F814W or F606W data (single-filter) and the ones found in both filters (multi-filter candidates).

large-scale sensitivity variations across the instrument's field of view. For each source we use all other sources within a $20''$ radius to determine the local correction for that source and visit. The local correction is the median difference between the magnitude predicated by the robust linear fit to the light-curve, and that actually measured. Variability detection in the light-curves obtained with the same instrument and filter require maximising the relative precision, while the absolute photometric accuracy is of little concern.

We searched for a variability detection method that would be sensitive to a wide range of variability types, robust to outlier measurements, and applicable to light-curves with a small number of points (the last requirement rules out period search techniques). After comparing 18 'variability indices' discussed by Sokolovsky *et al.* (2017a) we selected a magnitude-dependent cut in Median Absolute Deviation (MAD) as our variability detection statistic. MAD is a robust measure of light-curve scatter (e.g., Zhang *et al.* 2016) defined as $\mathrm{MAD} = \mathrm{median}(|m_i - \mathrm{median}(m_i)|)$, where m_i is the ith magnitude measurement in a light-curve. For each group and each set of measurements obtained with the same instrument and filter we identify as candidate variables the light-curves whose MAD values are at least 5σ larger than the median MAD value at the source (median) magnitude. Here we rely on the assumption that the majority of field sources are not variable above the 1% level, so the ones that stand out in the MAD–magnitude plot (Fig. 1) are the variable sources (or sources measured with much lower accuracy than the majority of sources in that group).

Photometric errors reported in the HSC are often underestimated (Whitmore *et al.* 2016), but they are not expected to be overestimated. We require all candidate variables to have the reduced χ^2 value associated with the hypothesis that the candidate has constant brightness $\chi^2_{\mathrm{red}} > 3$ (Andrae *et al.* 2010). This helps us handle the cases where a particular object could not be measured well on account of high local background and which was correctly reflected in the error bars.

3. Preliminary Results

In our preliminary analysis based on the second version of the HSC, out of 1.85 million sources that passed the initial quality cuts for the variability search 52 000 (2.8%) were

marked as candidate variables; among those, 7,800 were identified as variable in more than one filter. The candidates have an AB magnitude range of 15–27^m (median 22^m).

We performed a visual inspection of all the candidate variables detected in multiple filters. For each candidate we inspected its light-curve, position in the colour–magnitude diagram, and the three images associated with the brightest, median and faintest brightness measurement. About 70% of the candidates passed our visual inspection with no obvious problems with their images (crowding, imaging artefacts) or similarities in their light-curves to those of other sources in the group (that may indicate systematics affecting the photometry of multiple sources). We noticed that some groups had unrealistically high numbers of candidates that showed large scatter in their light-curves. The problem was traced to a slight misalignment between the white-light images used to detect sources and place the measuring apertures, and the filter-combined images used to obtain measurements in a given filter. That misalignment will be eliminated in future HSC versions, but for the initial version of the HCV (based on the second version of the HSC) the fields severely affected by misalignment had to be excluded from the analysis.

We continue to improve our candidate selection and validation criteria. The initial release of the HCV will include the clean sample of variables detected in multiple filters and validated by human experts, as well as the extended list of candidate variables detected by the automated selection only. The HCV will be released in 2019.

Acknowledgements

References

Anderson, J., & van der Marel, R. P. 2010, *ApJ*, 710, 1032
Andrae, R., Schulze-Hartung, T., & Melchior, P. 2010, arXiv:1012.3754
Bellini, A., Anderson, J., & Bedin, L. R. 2011, *PASP*, 123, 622
Bertin, E., & Arnouts, S. 1996, *A&AS*, 117, 393
Brown, T. M., Ferguson, H. C., Smith, E., *et al.* 2004, *AJ*, 127, 2738
Budávari, T., & Lubow, S. H. 2012, *ApJ*, 761, 188
Czerny, B., Beaton, R., Bejger, M., *et al.* 2018, *Space Sci. Rev*, 214, #32
Freedman, W. L., Madore, B. F., Gibson, B. K., *et al.* 2001, *ApJ*, 553, 47
Gavras, P., Bonanos, A. Z., Bellas-Velidis, I., *et al.* 2017, in: M. Brescia *et al.* (eds.),
    Astroinformatics, *Proc. IAUS 325* (CUP: Cambridge, UK), p. 369
Hack, W. J., Dencheva, N., Fruchter, A. S., *et al.* 2012, *AAS* Meeting Abstracts #220, 135.15
Huang, C. D., Riess, A. G., Hoffmann, S. L., *et al.* 2018, arXiv:1801.02711
Jenkner, H., Doxsey, R. E., Hanisch, R. J., *et al.* 2006, *ADASS* XV, 351, 406
Koekemoer, A. M., Ellis, R. S., McLure, R. J., *et al.* 2013, *ApJS*, 209, 3
Lasker, B. M., Lattanzi, M. G., McLean, B. J., *et al.* 2008, *AJ*, 136, 735
Nascimbeni, V., Bedin, L. R., Heggie, D. C., *et al.* 2014, *MNRAS*, 442, 2381
Riess, A. G., Rodney, S. A., Scolnic, D. M., *et al.* 2018, *ApJ*, 853, 126
Sokolovsky, K. V., Gavras, P., Karampelas, A., *et al.* 2017, *MNRAS*, 464, 274
Sokolovsky, K., Bonanos, A., Gavras, P., *et al.* 2017, in: M. Catelan & W. Gieren (eds.), *Wide-
    Field Variability Surveys: A 21st Century Perspective*, *EPJ Web of Conferences*, 152, 02005
Whitmore, B., Lindsay, K., & Stankiewicz, M. 2008, *ADASS* XVII, 394, 481
Whitmore, B. C., Allam, S. S., Budávari, T., *et al.* 2016, *AJ*, 151, 134
Yang, M., Bonanos, A. Z., Gavr as, P., *et al.* 2017, arXiv:1711.11491
Zhang, M., Bakos, G. Á., P enev, K., *et al.* 2016, *PASP*, 128, 035001